Progress In Electromagnetics Research M, Vol. 115, 141–149, 2023

Performance Evaluation of Biophotonic Cholesterol Sensor Using 1D Photonic Crystal Cavity Structure

Diptimayee Dash and Jasmine Saini*

Abstract—An efficient biochemical sensor for the detection of cholesterol concentration using a 1-dimensional photonic crystal (1D-PhC) based cavity structure has been proposed in this paper. The structure comprises 1-dimensional alternating dielectric photonic crystal designed as $(A/B)^2/D_d/(A/B)^2$ for measuring cholesterol concentration in blood, where 'A' and 'B' represent high and low refractive index materials, respectively. A cavity containing the cholesterol is inserted in the middle of the structure to assess its concentration. The transfer matrix method is used to analyze the reflection characteristics of the proposed multilayer structure. Sensitivity is analyzed by taking the difference in shifted resonant wavelength by infiltrating varying cholesterol concentrations ranging from 200 to 300 mg/dl. After rigorous optimization, it has been observed that the maximum sensitivity of 2.9 nm/(mg/dl) or 325 nm/RIU can be achieved.

1. INTRODUCTION

The leading factor in fatalities worldwide is cardiovascular disease (CVD). An estimated 17 million people die annually from CVD. The increasing total cholesterol concentration and triglyceride content in blood plasma are major risk factors. Cholesterol molecule is often found in the bloodstream and comprises lipids and proteins [1]. Varying protein and lipid ratios determine whether cholesterol is good or bad. Cell membranes and hormone production are both derived from cholesterol. The body's primary source of cholesterol is the liver. The increase in the cholesterol concentration above the normal range causes many fatal diseases like atherosclerosis (a condition due to the deposition of cholesterol inside the arteries in the human body) [2], cardiovascular disease (a disease that occurs due to faulty performance of heart and blood vessels, like heart attack, stroke), hypercholesterolemia, etc. [3]. The most common method of determining blood cholesterol is to measure the total amount of cholesterol in milligrams per deciliter of blood (mg/dl). A range of 200 mg/dl or less is regarded as the standard for total cholesterol levels. A borderline high for heart disease is assessed to have a total cholesterol level of 200 to 239 mg/dl. A person with a total cholesterol level of more than 240 mg/dl is twice as likely to develop heart disease as someone with a cholesterol level of under 200 mg/dl [4]. The body's cholesterol levels are a good indicator of cardiovascular health. Additionally, regular cholesterol monitoring is recommended because elevated cholesterol levels do not cause any symptoms in the human body. In the literature, several sensors have been designed and implemented to measure total cholesterol levels using cholesterol oxidase (ChOx). Nguyes et al. [5] reported a graphene-based electrochemical microelectrode-based structure to measure cholesterol levels with a sensitivity of 74 $\mu AmM^{-1}cm^{-2}$. The authors have used a multilayer structure of PANi/Fe_3O_4/graphene along with a layer of immobilized Cholesterol oxidase. Budiyanto et al. [6] used a He-Ne laser-based fiber optic system for cholesterol concentration measurement. They reported a 0.0004 mV/ppm average sensitivity in the range of 0 ppm to 300 ppm.

Received 25 January 2023, Accepted 23 February 2023, Scheduled 6 March 2023

* Corresponding author: Jasmine Saini (jasmine.saini@jiit.ac.in).

The authors are with the Jaypee Institute of Information Technology, Department of Electronics & Communication Engineering, Noida-62, India, 201309.

In [7], a photonic crystal fiber-based optrode was proposed to measure the total cholesterol levels. A thin film mixed with cholesterol enzyme was designed to be deposited at one side of the photonic crystal fiber. This procedure offered a good relationship between cholesterol concentration and the light intensity with the help of an optrode. Recently, the potential of the photonic crystal technique has been explored widely for designing label-free bio-chemical sensors with low detection limits [8–10], high sensitivity [11, 12] and selectivity to detect the target element for real-time monitoring. Due to their low cost and compact size, photonic crystal biosensors have emerged as potential candidates in this research area [13–16]. A number of bio-sensors have been proposed using PhC technology [17–23]. However, cholesterol concentration measurement has not been carried out using PhC techniques. The present work emphasizes exploring the potential of PhC cavity structure for cholesterol concentration measurement. A theoretical design of a 1D-biophotonic crystal cavity structure has been proposed and optimized using the Transfer Matrix Method (TMM). The obtained results are validated using COMSOL Multiphysics. Infiltration of various cholesterol concentrations (200 mg/dl–300 mg/dl) leads to a shift in resonance wavelength of the PhC cavity. It has been found that the resonant wavelength shifts in accordance with cholesterol concentration using the proposed design, yielding a higher value of sensitivity. By detecting the change in resonant wavelength with respect to cholesterol concentration, it is possible to achieve a good sensitivity of 2.9 nm/(mg/dl) or 325 nm/RIU. This exhibits the design's potential for use in the medical industry.

2. PROPOSED STRUCTURE

The proposed 1D-PhC cavity model uses alternate layers of high refractive index (n_h) and low refractive index (n_l) material. A defect layer of refractive index (n_d) is introduced in the middle of the alternating layers as presented in Fig. 1(a). The proposed structure possesses periodicity along the z-axis, and it is homogeneous in the x direction. Hence, the characteristic equation of the refractive index can be written as

$$n(z) = \begin{cases} n_h & 0 < z < D_h \\ n_l & D_h < z < D_h + D_l \end{cases}$$

where D_h and D_l are the thicknesses of high and low refractive index dielectric materials, and the z-axis is perpendicular to the multilayer structure. When the EM waves are incident on the periodic multilayer structure, some of the photons are reflected, and some are propagated through the photonic crystal. A photonic bandgap forms when a particular frequency wave is incident onto it. The reflection response of the proposed structure is calculated using Transfer Matrix Method [24, 25]. For multiple dielectric layers, let there be N number of dielectric layers and $N+1$ interfaces. Thus, the reflection spectra are calculated using the product of all single-layer transfer matrices. The overall reflection response Γ can be calculated as $\Gamma = \frac{E_-}{E_+}$, where E_+ and E_- are the forward and backward electric fields, respectively. For each layer, the relationship between the total electric field and the transfer matrix is derived as

$$\begin{bmatrix} E_p \\ H_p \end{bmatrix} = \begin{bmatrix} \cos k_p l_p & j\eta_p \sin k_p l_p \\ j\eta_p^{-1} \sin k_p l_p & \cos k_p l_p \end{bmatrix} \begin{bmatrix} E_{p+1} \\ H_{p+1} \end{bmatrix} \quad \text{Where } p = N,\ N-1,\ \ldots,\ 1.$$

and

$$\Gamma_p = \frac{\rho_p + \Gamma_{p+1} e^{-2jk_p l_p}}{1 + \rho_p \Gamma_{p+1} e^{-2jk_p l_p}}$$

where l_p is the distance between the two interfaces, and $k_p l_p$ is the phase thickness of the p^{th} dielectric layer.

3. STRUCTURE ANALYSIS AND RESULTS

The proposed geometry is developed by inserting a defect layer 'D_d' between two uniform 1D-PhC structures. Glass (BK 7) with a refractive index of 1.5 is taken as the substrate layer. The structure is composed of substrate/$(A/B)^M/D_d/(A/B)^M$/Air, where 'M' is the number of periodic

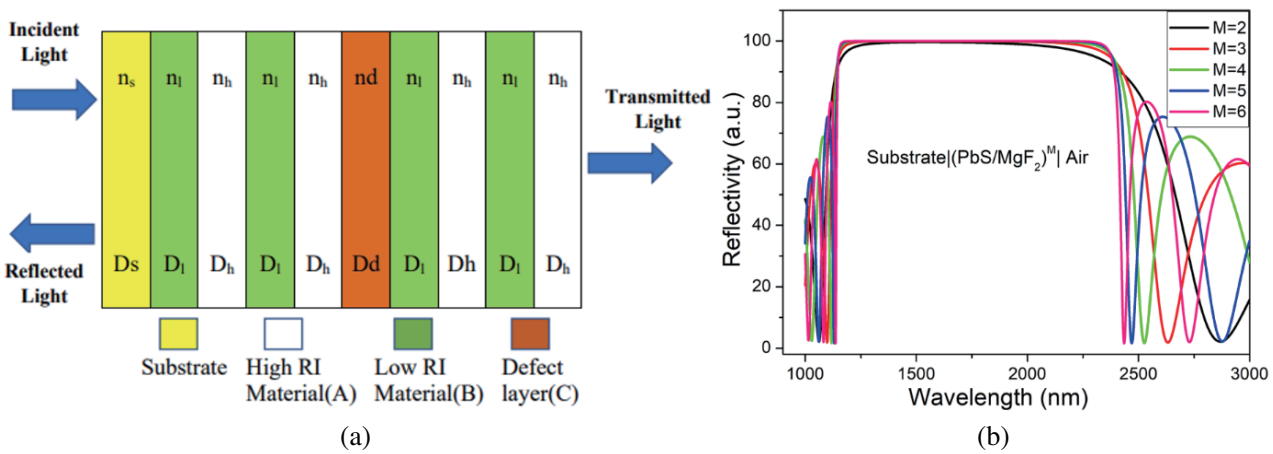

Figure 1. (a) Schematic diagram of proposed 1D photonic crystal with middle defect layer and (b) Reflection spectrum variation for Substrate/$(A/B)^M$/Air structure as a function of 'M'.

dielectric materials as shown in Fig. 1(a). The proposed 1D photonic crystal is designed by using 'A' as high refractive index dielectric material having a refractive index $(n_h) = 4.2$. The thickness $(D_h) = (\lambda/4 \times n_h)$ is calculated using Bragg's Reflector formula, considering 1550 nm as resonating wavelength. Similarly, low refractive index dielectric material 'B' having refractive index $n_l = 1.38$ and thickness $D_l = (\lambda/4 \times n_l)$ is considered in the proposed design.

Initially, a 1D-PhC structure substrate/$(A/B)^M$/Air is considered. The structure has been optimized to achieve 100% reflectivity with 'M' number of layers. This gives the two multilayer stacks itself as an optimized design. The measured reflection spectrum has a lower edge at 1062 nm and an upper edge at 2900 nm. This gives a photonic bandgap around 1838 nm having a central wavelength around 1550 nm.

The same has been represented in Fig. 1(b). The wider photonic bandgap is formed because of higher refractive index contrast between the 'A' and 'B' layers. The defect layer is inserted in the middle of the structure (orange colour layer in Fig. 1(a)). Initially, the defect layer is considered with a refractive index of n_h and length D_h. The introduction of a defect layer results in a razor-sharp dip in the reflectivity, as evident from Fig. 2(a). Fig. 2(b) represents the surface electric field profile of

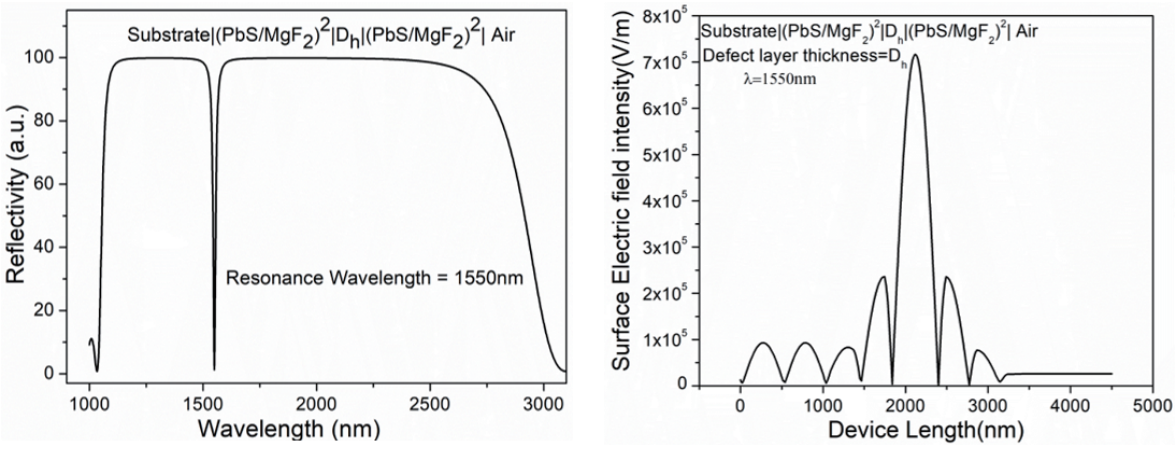

Figure 2. (a) Reflection spectrum for Substrate/$(A/B)^2/D_h/(A/B)^2$/Air and (b) Surface electric field profile of structure with defect layer thickness D_h at resonant wavelength of 1550 nm.

structure "Substrate/$(A/B^2/D_h/(A/B)^2$/Air" with defect layer thickness D_h at resonant wavelength of 1550 nm.

Therefore, considering cholesterol concentration (200 mg/dl) as a defect layer results in blue shifting of peak resonance wavelength to around 1330 nm. This resonance wavelength can be tailored to the desired wavelength by varying the defect layer thickness and defect layer refractive index. Figure 3 illustrates the variation in the thickness of the defect layer, ranging from D_h to $3D_h$, and the impact on the layer made up of cholesterol with a concentration of 200 mg/dl.

Figure 3 shows the effect of varying the defect cholesterol layer width on resonance wavelength. With increasing the defect layer thickness, a red shift in resonance wavelength has been observed. Similarly, infiltration of higher cholesterol concentration (at fixed D_h) also exhibits higher resonance wavelength. The measurement of cholesterol concentration is carried out by comparing the obtained resonance wavelength shift with the normal concentration level (200 mg/dl). The refractive indices of different cholesterol concentrations have been experimentally obtained using the Z-scan technique [26, 27] and are represented in Table 1.

The distance between resonating modes is observed to increase as the defect layer's width increases, even though the refractive index changes slightly. The proposed bio-photonic sensor's sensitivity is thus enhanced.

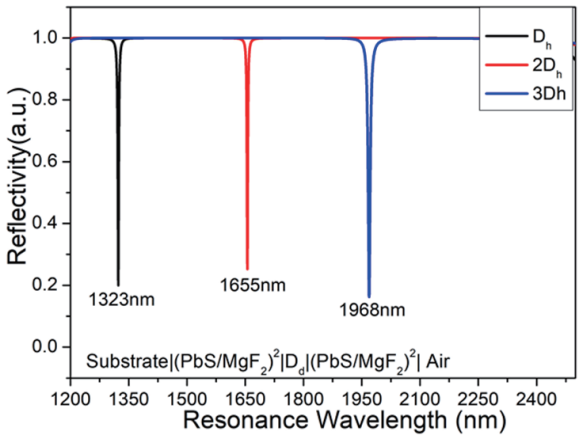

Figure 3. Variation of reflectivity versus resonance wavelength at different widths of defect layer for Substrate/$(A/B)^2/Dd/(A/B)^2$/Air structure.

Table 1. Refractive index value for cholesterol concentration.

Standard Cholesterol Concentration (mg/dl)	Refractive index
200	2.49 ± 0.08
220	2.62 ± 0.09
240	2.80 ± 0.07
260	3.06 ± 0.06
280	3.23 ± 0.07
300	3.47 ± 0.09

Sensitivity of the sensor is measured as the ratio of change in position of defect mode wavelength ($\Delta\lambda_d$) in defect layer to corresponding change in refractive index (Δn_d) of analyte infiltration against normal cholesterol concentration (200 mg/dl). Sensitivity of the sensor is expressed by $S = \frac{\Delta\lambda_d}{\Delta n_d}$. Apart from sensitivity, some other sensor parameters are calculated and presented in Table 3. The detection

Table 2. Sensitivity of different cholesterol concentrations at different widths of defect layers.

Cholesterol Concentration (mg/dl)	**Sensitivity (nm/RIU)**				
	$D_d = D_h$	$D_d = 1.5D_h$	$D_d = 2D_h$	$D_d = 2.5D_h$	$D_d = 3D_h$
220	123.0769	200	276.9231	323.0769	369.2308
240	125.8065	200	264.5161	312.9032	348.3871
260	129.8246	205.2632	256.1404	301.7544	315.7895
280	129.7297	202.7027	252.7027	298.6486	300
300	132.6531	200	245.9184	290.8163	293.8776

Table 3. Sensitivity, signal to noise ratio, detection limit, sensor resolution, and figure of merit of proposed graded refractive index sensor at various cholesterol concentrations and defect layer thickness of $3D_h$.

Cholesterol concentration (mg/dl)	**S (nm/RIU)**	**Quality Factor**	**Detection limit**	**Sensor resolution**	**FOM ($\mathbf{RIU^{-1}}$)**
220	369.2308	328.1666667	0.006646953	2.45425995	61.53846667
240	348.3871	251.5	0.008095743	2.82045232	43.5483875
260	315.7895	413.8	0.01156989	3.653649857	63.1579
280	300	429	0.0129501	3.885030096	60
300	293.8776	274.25	0.012469915	3.66462869	36.7347

limit (DL) is the smallest refractive index change that our sensor is capable of detecting; it is determined by the ratio of sensor's resolution to sensitivity as given by [28]: $DL = \frac{SR}{S}$. The smallest spectral shift that may be observed is called sensor resolution (SR), and it is provided by $SR = \frac{\text{FWHM}}{1.5(SNR)^{0.25}}$, where full width half maximum (FWHM) is the spectral half width of the resonant wavelength dip, and quality factor is given as: $QF = \frac{\lambda_r}{\text{FWHM}}$, where λ_r is the resonant wavelength. The calculation of the figure of merit [2] (FOM) involves determining the ratio between sensitivity and full width at half maximum (FWHM) as expressed by the formula: $FOM = \frac{S}{\text{FWHM}}$.

In the current simulations, the defect layer thickness is varied from D_h to $3D_h$ with the step of 0.5. The further increase in defect layer thickness does not have much effect on sensitivity. Therefore, the defect layer thickness up to $3D_h$ is considered in the current optimization. The sensitivity probing of the proposed geometry for various defect layer widths is shown in Fig. 4. Fig. 4(a) illustrates the reflection spectrum for the defect layer thickness of D_h (94.29 nm). The defect layer is infiltrated with a cholesterol concentration of 200 mg/dl to 300 mg/dl with the step of 20. This gives average sensitivity of 128.2181 nm/RIU. The same process has been repeated for the defect layer thicknesses of $1.5D_h$ (128.2181 nm), $2D_h$ (184.58 nm), $2.5D_h$ (230.72 nm), $3D_h$ (276.87 nm), and corresponding reflection spectrums are shown in Figs. 4(b)–(e), respectively. This gives the corresponding average sensitivity of around 201.5932 nm/RIU, 259.2401 nm/RIU, 305.4399 nm/RIU, and 325.457 nm/RIU. As the value of cavity thickness is increasing, the defective modes shift towards longer wavelength regions. Fig. 4(f) shows the comparative sensitivity analysis for various defect layer thicknesses, and the analysis is summarized in Table 2.

Table 2 presents the impact of increasing the defect layer width upon the sensitivity. A higher sensitivity of around 369.23 nm/RIU is achieved when the width of the defect layer is at $3D_h$ at normal incidence. From the above table, it is observed that with an increase in the defect layer width,

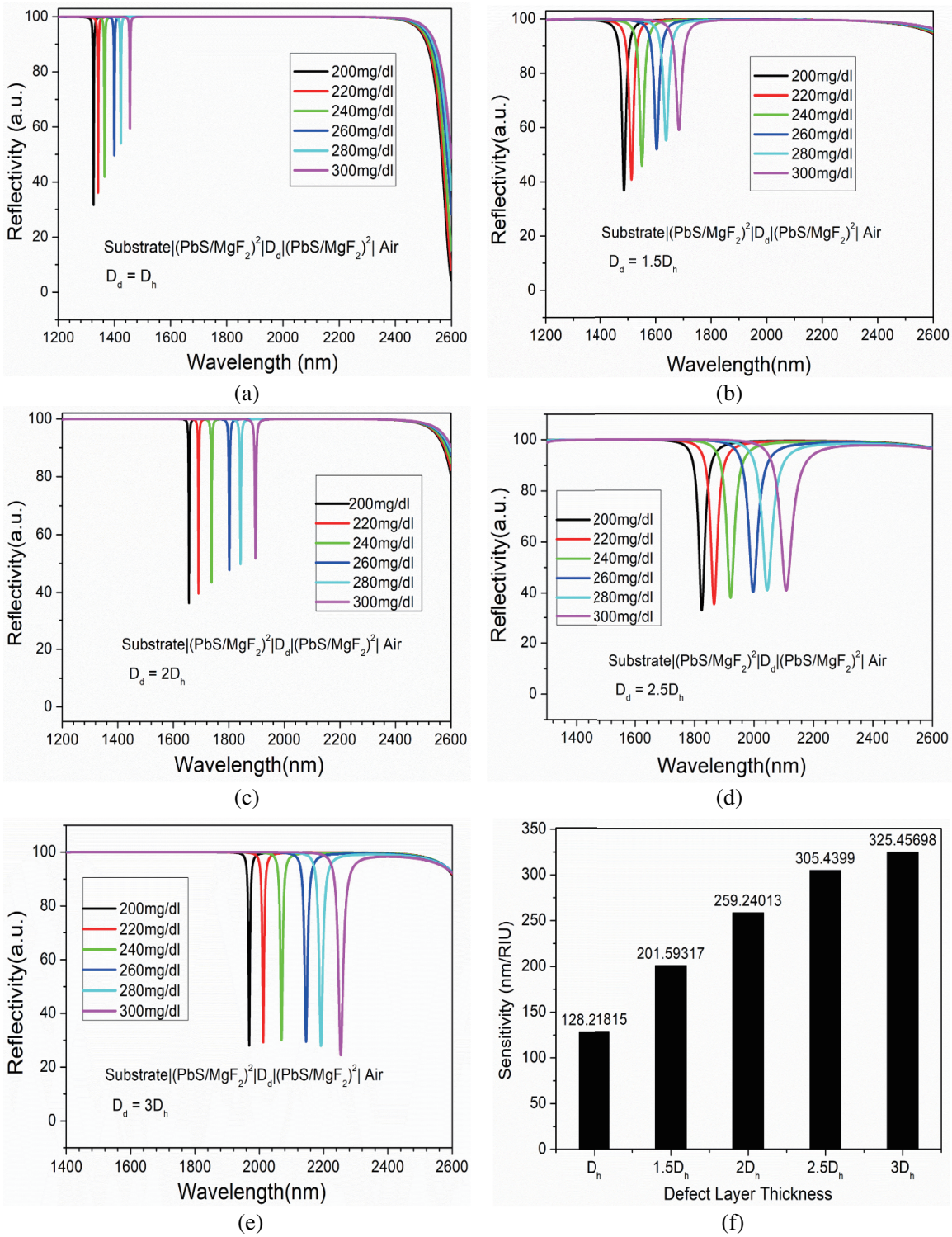

Figure 4. Effect of varying defect layer thicknesses on sensitivity for the structure Substrate/$(A/B)^2/D_d/(A/B)^2$/Air, (a) $D_d = D_h$, (b) $D_d = 1.5D_h$, (c) $D_d = 2d_h$, (d) $D_d = 2.5D_h$, (e) $D_d = 3D_h$, and (f) corresponding sensitivity comparison.

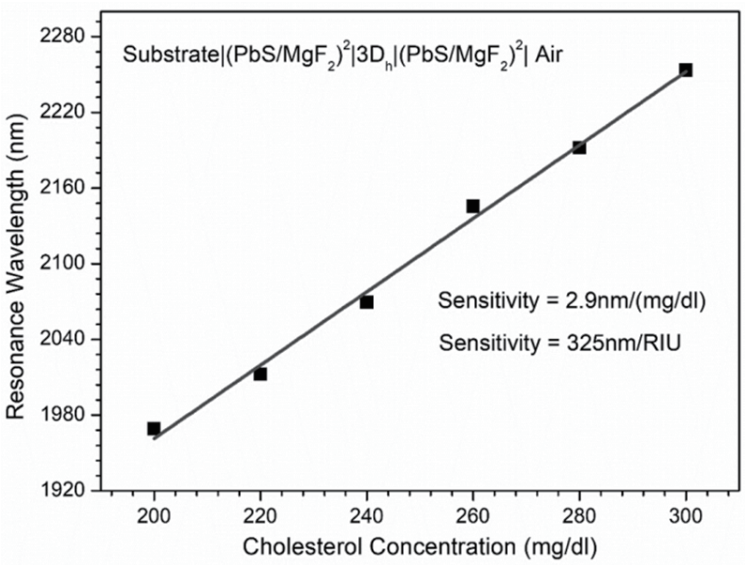

Figure 5. Variation of resonance wavelength by infiltrating different cholesterol concentrations in the defect layer for Substrate/$(A/B)^2/3D_h/(A/B)^2$/Air structure.

sensitivity also increases. However, the sensitivity decreases for higher cholesterol concentration values. For a cholesterol concentration of 300 mg/dl, the maximum sensitivity is around 293.87 nm/RIU at a defect layer thickness of $3D_h$. Fig. 5 illustrates the results of a thorough sensitivity analysis of the Substrate/$(A/B)^2/3D_h/(A/B)^2$/Air structure, in detail.

At the defect layer thickness of $3D_h$, an infiltration with cholesterol concentration from 200 mg/dl to 300 mg/dl is done. It is observed that the resonant wavelength linearly increases from 1968 nm to 2256 nm with a linear fitted equation: $\lambda = 2.90886*$ Cholesterol concentration + 1379.68571. An average sensitivity around 2.9 nm/(mg/dl) or 325 nm/RIU, along with a standard correlation error coefficient (R) about 0.0997, has been achieved. The proposed structure exhibits the average detection limit of 1.03×10^{-2}, average quality factor of 3.39×10^2, and average figure of merit 52.9 RIU^{-1}. Finally, Table 4 represents a comparative analysis of the proposed optimized geometry with the latest stated results in the literature in terms of their sensing capability.

Table 4. A comparative analysis of proposed structure with latest developed application-based sensors.

Application	Sensitivity (nm/RIU)	Year	Reference
Detection of reproductive female hormones	137.02	2021	[29]
Dengue virus detection sensor	203.09	2022	[30]
Detection of water concentration in ethanol solution	144.369	2022	[31]
Detection of Fat Concentrations in Milk	214.28	2022	[32]
Proposed Cholesterol Sensor	325 nm/RIU or 2.9 nm/(mg/dl)	proposed work	

4. CONCLUSION

In this work, an efficient and compact refractive index-based bio-photonic cholesterol sensor using a 1D photonic crystal cavity structure has been proposed to measure the cholesterol level in the blood. The performance study is carried out using TMM method. A thorough analysis of the impact of varying defect layer width and refractive index is performed in detail. After rigorous optimization, a remarkably high sensitivity of 325 nm/RIU or 2.9 nm/(mg/dl) is obtained. Thus, the proposed structure shows its potential applications in biochemical sensing applications.

REFERENCES

1. Soliman, G. A., "Dietary cholesterol and the lack of evidence in cardiovascular disease," *Nutrients*, Vol. 10, No. 6, MDPI AG, 2018, [doi:10.3390/nu10060780].
2. Russell, R., "Atherosclerosis-an inflammatory disease," *N. Engl. J. Med.*, Vol. 340, 115–126, 1999, [doi: 10.1056/NEJM199901143400207].
3. Soutar, A. K. and R. P. Naoumova, "Mechanisms of disease: Genetic causes of familial hypercholesterolemia," *Nature Clinical Practice Cardiovascular Medicine*, Vol. 4, No. 4, 2007, [doi:10.1038/ncpcardio0836].
4. McNamara, D. J., "Dietary cholesterol and atherosclerosis," *Biochimica et Biophysica Acta — Molecular and Cell Biology of Lipids*, Vol. 1529, 1–3, 2000, [doi:10.1016/S1388-1981(00)00156-6].
5. Nguyen, H. B., H. D. Le, V. Q. Nguyen, T. T. T. Ngo, Q. P. Do, X. N. Nguyen, and N. M. Phan, "Development of the layer-by-layer biosensor using graphene films: Application for cholesterol determination," *Advances in Natural Sciences: Nanoscience and Nanotechnology*, Vol. 4, No. 1, 2013, [doi:10.1088/2043-6262/4/1/015013].
6. Budiyanto, M., Suhariningsih, and M. Yasin, "Cholesterol detection using optical fiber sensor based on intensity modulation," *Journal of Physics: Conference Series*, Vol. 853, No. 1, 2017, [doi:10.1088/1742-6596/853/1/012008].
7. Razo-Medina, D. A., E. A. Méndez, and M. T. Durán, "Thin film of sol-gel deposited in photonic crystal fiber for cholesterol detection," *Nanosensors, Biosensors, and Info-Tech Sensors and Systems*, Vol. 9434, 2015, [doi:10.1117/12.2084280].
8. Goyal, A. K., A. Kumar, and Y. Massoud, "Thermal stability analysis of surface wave assisted bio-photonic sensor," *Photonics*, Vol. 9, No. 5, 324, 2022, [doi: 10.3390/photonics9050324].
9. Goyal, A. K. and J. Saini, "Performance analysis of Bloch surface wave-based sensor using transition metal dichalcogenides," *Applied Nanoscience (Switzerland)*, Vol. 10, No. 11, 2020, [doi:10.1007/s13204-020-01538-0].
10. Goyal, A. K., H. S. Dutta, and S. Pal, "Development of uniform porous one-dimensional photonic crystal based sensor," *Optik (Stuttg)*, Vol. 223, 2020, [doi:10.1016/j.ijleo.2020.165597].
11. Nouman, W. M., S. E-S. Abd El-Ghany, S. M. Sallam, A.-F. B. Dawood, and A. H. Aly, "Biophotonic sensor for rapid detection of brain lesions using 1D photonic crystal," *Opt Quantum Electron*, Vol. 52(6) (2020) [doi:10.1007/s11082-020-02409-2].
12. Goyal, A. K., "Design analysis of one-dimensional photonic crystal-based structure for hemoglobin concentration measurement," *Progress In Electromagnetics Research M*, Vol. 97, 2020, [doi:10.2528/pierm20080601].
13. Dash, D., J. Saini, A. K. Goyal, and Y. Massoud, "Exponentially index modulated nanophotonic resonator for high-performance sensing applications," *Scientific Report*, Vol. 13, 1431, 2023, [https://doi.org/10.1038/s41598-023-28235-6].
14. Robertson, W. M. and M. S. May, "Surface electromagnetic wave excitation on one-dimensional photonic band-gap arrays," *Appl. Phys. Lett.*, Vol. 74, No. 13, 1800–1802, American Institute of Physics Inc., 1999, [doi:10.1063/1.123090].
15. Goyal, A. K., H. S. Dutta, and S. Pal, "Porous photonic crystal structure for sensing applications," *J. Nanophotonics*, *SPIE-Intl. Soc. Optical Eng.*, Vol. 12, No. 04, 1, 2018, [doi: 10.1117/1.jnp.12.040501].

16. Dutta, H. S., A. K. Goyal, and S. Pal, "Analysis of dispersion diagram for high performance refractive index sensor based on photonic crystal waveguides," *Photonics Nanostruct*, Vol. 23, 2017, [doi: 10.1016/j.photonics.2016.11.004].
17. Goyal, A. K., H. S. Dutta, and S. Pal, "Performance optimization of photonic crystal resonator based sensor," *Optical and Quantum Electronics*, Vol. 48, 431, 2016, [doi: 10.1007/s11082-016-0701-0].
18. Panda, A. and P. D. Pukhrambam, "Analysis of GaN-based 2D photonic crystal sensor for real-time detection of alcohols," *Brazilian Journal of Physics*, Vol. 51, No. 3, 481–492, Springer, 2021, [doi:10.1007/s13538-021-00856-0].
19. Aly, A. H., Z. A. Zaky, A. S. Shalaby, A. M. Ahmed, and D. Vigneswaran, "Theoretical study of hybrid multifunctional one-dimensional photonic crystal as a flexible blood sugar sensor," *Phys. Scr.*, Vol. 95, No. 3, Institute of Physics Publishing, 2020, [doi:10.1088/1402-4896/ab53f5].
20. Banerjee, A., "Enhancement in sensitivity of blood glucose sensor by using 1D defect ternary photonic band gap structures," *Journal of Optics*, Vol. 48, No. 2, India, 2019, [doi:10.1007/s12596-019-00521-5].
21. Goyal, A. K. and S. Pal, "Design analysis of Bloch surface wave-based sensor for haemoglobin concentration measurement," *Applied Nanoscience (Switzerland)*, Vol. 10, No. 9, 3639–3647, Springer Science and Business Media Deutschland GmbH, 2020, [doi:10.1007/s13204-020-01437-4].
22. Aly, A. H., D. Mohamed, M.A. Mohaseb, and N. S. Abd El-Gawaad, "Biophotonic sensor for the detection of creatinine concentration in blood serum based on 1D photonic crystal," *RSC Adv.*, Vol. 10, No. 53, 31765–31772, Royal Society of Chemistry, 2020, [doi:10.1039/d0ra05448h].
23. Goyal, A. K., H. S. Dutta, and S. Pal, "Design and analysis of photonic crystal micro-cavity based optical sensor platform," *AIP Conference Proceedings*, Vol. 1724, 2016, [doi:10.1063/1.4945125].
24. Yeh, P. and M. Hendry, "Optical waves in layered media," *Phys. Today*, Vol. 43, No. 1, 1990, [doi:10.1063/1.2810419].
25. Goyal, A. K., M. Husain, and Y. Y. Massoud, "Analysis of interface mode localization in disordered photonic crystal structure," *J. Nanophoton.*, Vol. 16, No. 4, 046007, 2022, [doi: 10.1117/1.JNP.16.046007].
26. Dhinaa, A. N. and P. K. Palanisamy, "Z-scan technique for measurement of total cholesterol and triglycerides in blood," *Journal of Innovative Optical Health Sciences*, Vol. 02, No. 03, 295–301, 2009, [https://doi.org/10.1142/S1793545809000565].
27. Edappadikkunnummal, S., R. C. Vasudevan, S. Dinesh, S. Thomas, N. R. Desai, and S. Kaniyarakkal, "Detection of hemoglobin concentration based on defective one-dimensional photonic crystals," *Photonics*, Vol. 9, No. 9, 660, 2022, [https://doi.org/10.3390/photonics9090660].
28. Pathania, P. and M. S. Shishodia, "Gain-assisted transition metal ternary nitrides (Ti1−xZrxN) core-shell based sensing of waterborne bacteria in drinking water," *Plasmonics*, Vol. 14, 1435–1442, 2019, https://doi.org/10.1007/s11468-019-00927-8.
29. Aly, A. H., S. K. Awasthi, A. M. Mohamed, M. Al-Dossari, Z. S. Matar, M. A. Mohaseb, N. S. Abd El-Gawaad, and A. F. Amin, "1D reconfigurable bistable photonic device composed of phase change material for detection of reproductive female hormones," *Phys. Scr.*, Vol. 96, No. 12, 125533, 2021, [doi: 10.1088/1402-4896/ac3efa].
30. Sharma, S. and A. Kumar, "Design of a biosensor for the detection of dengue virus using 1D photonic crystals," *Plasmonics*, Vol. 17, No. 2, 675–680, 2022, [https://doi.org/10.1007/s11468-021-01555-x].
31. Taya, S. A., A. Sharma, N. Doghmosh, and I. Colak, "Detection of water concentration in ethanol solution using a ternary photonic crystal-based sensor," *Materials Chemistry and Physics*, Vol. 279, 125772, 2022, [doi: 10.1016/j.matchemphys.2022.125772].
32. Panda, A. and P. D. Pukhrambam, "Study of metal-porous GaN-based 1D photonic crystal tamm plasmon sensor for detection of fat concentrations in milk," *Micro and Nanoelectronics Devices, Circuits and Systems*, Vol. 904, 415–425, 2022, [https://doi.org/10.1007/978-981-19-2308-1_42].